Provisionally accepted for publication

RESEARCH ARTICLE

Controlling delivery of Carbamazepine drug using multi walled carbon nanotubes

Majid **Mohammadi** [1,*], Mehdi **Vadi** [1], Narges **Bagehri** [1], Khadijeh **Shekoohi** [2]

[1] Department of Chemistry, Firoozabad Branch, Islamic Azad University, Firoozabad, Iran
[2] Department of Chemistry, Darab Branch, Islamic Azad University, Darab, Iran

[*] **Corresponding author**: Majedmohammadi63@gmail.com

ORCID: 0000-0001-6592-5934

Doi: 10.36118/pharmadvances.2023.52

SUMMARY

Todays, nanomaterial-based drug delivery systems can help to control the release of drugs. In this study, multiwalled carbon nanotubes (MWCNTs) were used as reliable carriers to enhance the delivery of carbamazepine (CBZ). The adsorption of the CBZ drugs on the MWCNTs was determined using three adsorption models, such as Langmuir, Freundlich, and Temkin. High values of isothermal constant (b) and separation factor (R_L) confirm strong and reliable adsorption of the CBZ drug with concentration of 60 mg L^{-1} at 303 Kelvin in acidic medium. Another important point is that the adsorption value decreases with increasing pH. The negative value of enthalpy (ΔH) based on Vant-Hoff equation shows that the adsorption of the CBZ drugs on the MWCNTs exhibits fast pseudo-first order kinetics and exothermic process in 90 minutes. Moreover, the negative value of Gibbs free energy (ΔG) shows that the adsorption

of the CBZ drug on the MWCNTs is a spontaneous process. Therefore, all the above parameters indicate that the MWCNTs can be considered as a reliable carrier for the adsorption, transfer, and controlled release of the CBZ drugs into the target cells with little side effects.

Key words: *exothermic process; isotherm models; multi walled carbon nanotube; carbamazepine drug; physical adsorption*.

Graphical Abstract (GA)

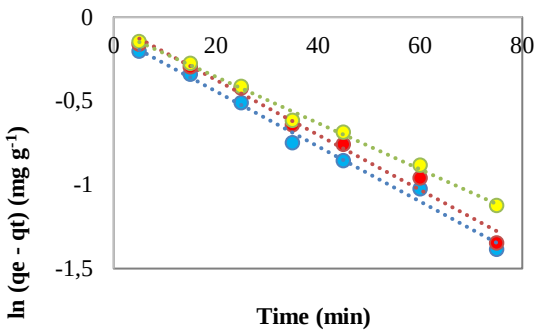

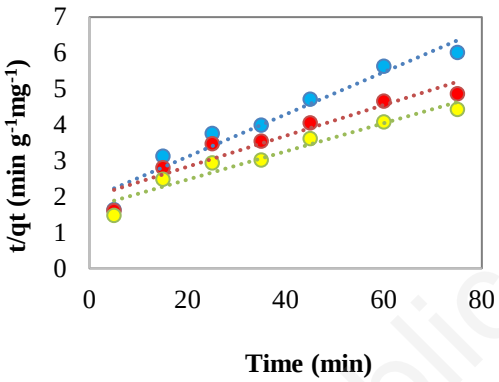

Pseudo-first order and pseudo-second order adsorption of Carbamazepine drug on multi walled carbon nanotube decreases and increases with increasing concentration.

Introduction

The selection of suitable carrier based on nanomaterials plays an important role in drug delivery. To achieve this, many research groups have proposed various carriers to deliver drugs into target cells[1–6]. In fact, drug molecules can combine with the carrier both chemically and physically under various conditions. One of the most advantageous carriers is CNTs because they have high surface-to-volume ratio, low density, and lower side effects.[7]

Multi-walled carbon nanotubes (MWCNTs) have been used for drug delivery because of their large surface area and low toxicity[8–13]. For example, this carrier has been used to enhance the controlled release of the insoluble drug dipyridamole[14]. In another study, MWCNTs were introduced for genetically modified Bifidobacterium longum because they can be transformed into a thick membrane[15]. MWCNTs are considered as a novel drug delivery system for the interaction of nutrient broth-treated (NBT) and cefotaxime sodium (CTX)[16]. In general, the interaction between drug and MWCNT carrier can be in different ways[17–20]. Therefore, in the current study, we will use MWCNTs as adsorbents for drug molecules.

The main topic of this study is to introduce reliable conditions for the adsorption of Carbamazepine (CBZ) drug as a tegretol, anticonvulsant, analgesic and to treat pain resulting from trigeminal neuralgia[21] on MWCNT with high applicability in drug delivery systems. Thus, the current work consists of the following steps: In the first step, we will interact the CBZ drug with MWCNTs to develop a model for favotable adsorption model. In the second step, we will investigate the adsorption isotherm in the best PH, temperature, etc.

The adsorption isotherm models

Langmuir model

The Langmuir model applies to single-layer adsorption of drugs on the adsorbent surface with equal and minimum adsorption position. Moreover, all adsorption sites without interaction

between adsorbed molecules are considered to be energetically equivalent[22]. The linear form of this model is expressed by the following equation:

$$\frac{C_e}{q_e} = \frac{1}{q_m b} + \frac{C_e}{q_m} \quad (1)$$

where q_e, C_e, q_m , and b are the amounts adsorbed from the solution, the concentration in solution at equilibrium and Langmuir constants, the constant representing the equilibrium adsorption capacity, the formation of a complete layer on the "th" surface of the adsorbent, and the equilibrium adsorption constant, respectively.

In addition, , the value of the separation factor value (R_L) is defined as an important point of the Langmuir model by means of the following equation[23]:

$$R_L = \frac{1}{1+bC_0} \quad (2)$$

Freundlich model

This model is based on single-layer adsorption at heterogeneous adsorption positions that are not the same and do not have the same energies. This assumption is in contrast to the Langmuir isotherm, which assumes that the enthalpy of adsorption is independent of the amount adsorbed on the surface [24]. The linear Freundlich equation is given by

$$lnq_e = lnK_F + \frac{1}{n} lnC_e \quad (3)$$

where K_F and n are constants of adsorption capacity and experimental dimensionless parameters related to adsorption intensity.

Temkin model

The experimental Temkin isotherm accounts for the interaction between adsorbate and adsorbent. In this model, adsorption is characterized by a uniform distribution of binding energies up to a maximum binding energy. The linear form of the Temkin model is expressed as follows:

$$q_e = B\ln A + B\ln C_e; \qquad B = \frac{RT}{b} \tag{4}$$

where B is a dimensionless constant with respect to the heat of adsorption, R (8.314 J mol^{-1} K^{-1}) is the ideal gas constant, T (K) is the absolute temperature, b (J mol^{-1}) is the isotherm Temkin constant and A (L g^{-1}) is the equilibrium binding constant with respect to the maximum binding energy [24].

Pseudo-first-order and pseudo-second-order models

These models identify the key process controlling the adsorption rate in physisorption and chemisorption, respectively. In the pseudo-first-order model, physisorption limits the adsorption rate of the particles onto the adsorbent, while the pseudo-second-order model, chemisorption is considered as the rate-limiting mechanism of the process[25].

Experimental

The MWCNT (weight 5g; OD 10-20 nm; length 30 µm; purity > 95 wt%; true density 2.1 g/cm^3) and the CBZ (86% purity) were purchased from Neutrino Company, Spain and Sobhan drug Company, Iran, respectively. The starting point of the experiment is the preparation of a stock solution (100 mg L^{-1}) by dissolving 0.05 g of CBZ in 500 ml of deionized water. The so-called working solutions of the drug are prepared at 20-60 mg L^{-1} from the primary concentration with deionized water.

In the second step, 10 ml of each concentration and 10 mg of the MWCNT were mixed together. The obtained samples were shaken on a magnetic stirrer (Heidolph, model Mr3001) at 1000 rpm for 90 min in 30 ℃. Then, each sample was centrifuged at 10,000 rpm for 10 min. The concentration of free CBZ in the solution was determined by recording the absorbance (λ_{max} = 205.2 nm) of the supernatant with a UV-Vis spectrophotometer (Perkin Elmer, Lambda5). The

absorbance values of some different CBZ concentrations were recorded. The pH of the solutions was simultaneously monitored with a pH meter (Metrohm 692 pH Meter, Herisau, Switzerland) and adjusted by adding HCl or NaOH solution. A scanning electron microscope (model TESCAN Vega3) and a transmission electron microscope (TEM) (PHILIPS EM 208S, 100 Kv, Netherlands) were used to obtain scanning electron microscopic (SEM) images.

Results and Discussion

In this study, the morphology of MWCNT and CBZ was investigated using SEM before and after adsorption of the drug onto MWCNT, see Figure 1. According to Figure 1.a, the morphology of MWCNT corresponds to 10-20 nm and 1-2 μm in diameter and length, respectively. Moreover, the TEM image shows the nature and purity of MWCNT and confirms the SEM data. Black and white colors on the inside and outside of the MWCNT mean that CBZ adsorption has occurred on the MWCNT nanotube.

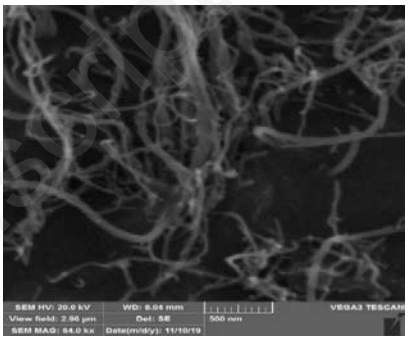

(a)

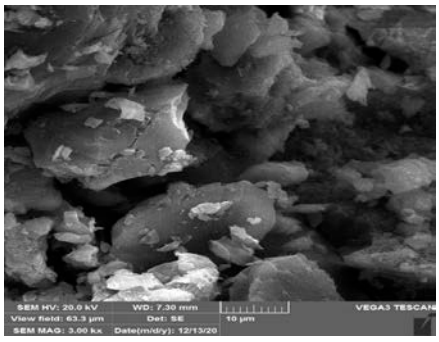

(b)

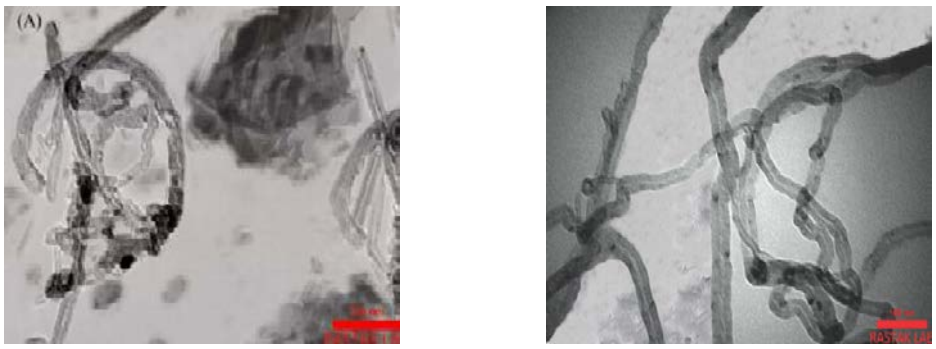

(c) (d)

Figure1. Scanning electron microscopy (SEM) images were achieved for multi-walled carbon nanotube MWCNT (a), the Carbamazpine (CBZ) (b) and transfer electron microscopy (TEM) images for the MWCNT (c), MWCNT-CBZ complex (d), respectively.

The equilibrium adsorption isotherms

The Langmuir model was plotted for temperatures 303, 308, and 318 K, respectively, to obtain the parameters equations by plotting $\frac{C_e}{q_e}$ vs. C_e (see Figure 2). According to this figure, in the linear line based on this model, maximum regression parameter (R^2), solution concentration (q_m) in mg g^{-1} is in 303 K temperature, see Table 1. All parameters show that the interaction of CBZ drug with MWCNT is based on electrostatic interaction. According to Table 1, the maximum value of the b (L mg^{-1}) at the 303 K shows that adsorption at this temperature is stronger than other temperatures.

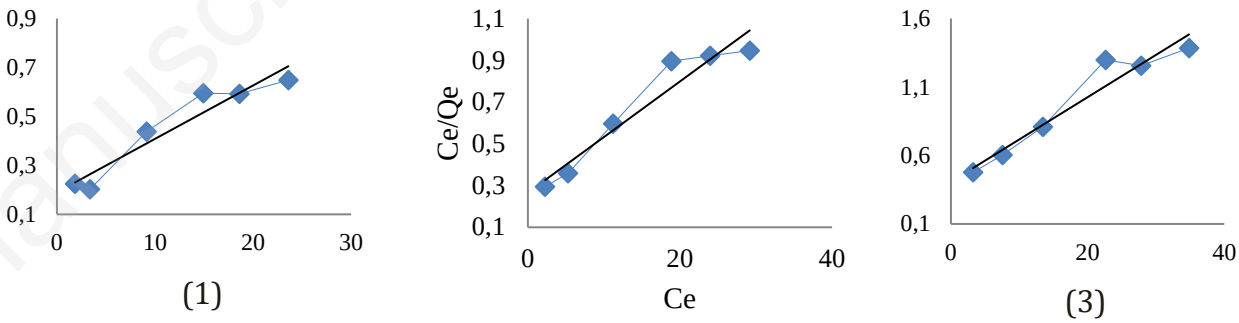

Figure 2. The equilibrium adsorption isotherm for the CBZ adsorption on the MWCNT in 303 (1), 308 (2), and 318 (3) K temperatures, respectively.

Table 1. The CBZ surface adsorption parameters based on Langmuir model.

Temperature (K)	R^2	b (L mg^{-1})	q_m (mg g^{-1})
303	0.935	0.115	45.87
308	0.931	0.101	37.47
318	0.919	0.076	32.36

The value of the separation factor (R_L) shows that the adsorption process is favorable or unfavorable, see Table 2. According to this table, the R_L value is close to zero, indicating good and favorable adsorption.

The R_L value for the adsorption of the CBZ drug on the MWCNT at three temperatures and six concentrations is shown in Figure 3. According this figure, the R_L value decreases with increasing the CBZ drug concentration; the minimum value of the R_L factor is observed at 60 mg L^{-1}. On the other hand, the minimum value of the R_L factor is at 303 K when temperatures are compared. The R_L value in the range of 0.0- 0.6 shows favorable adsorption at this temperature.

Table 2. Adsorption process type based on separation factor in Langmuir model.

R_L **value**	Adsorption process
$R_L > 1$	unfavorable
$R_L = 1$	linear
$0 < R_L > 1$	favorable
$R_L = 0$	irreversible

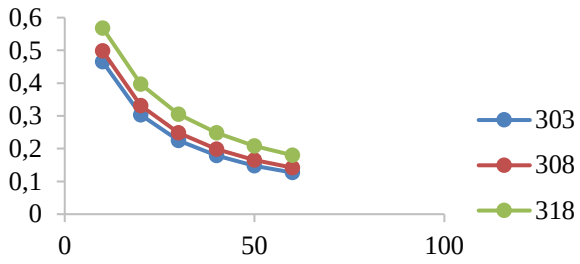

Figure 3. The R_L vs. the CBZ drug concentrations diagram for its adsorption on the MWCNT at three temperatures.

Freundlich model

As the constants of adsorption capacity (K_F) increases, the adsorption capacity for the CBZ drug increases. Moreover, the n value in the range of 0.0 – 1.0 shows that the adsorption process is favorable. If this value is close to 1.0 value, the heterogeneous surface area is of little importance; however, if it is above 1.0, it is more important.Therefore, the lnq_e vs. lnC_e plot is a straight line with $\frac{1}{n}$ slope and lnK_F intercept, respectively, see Figure 4.

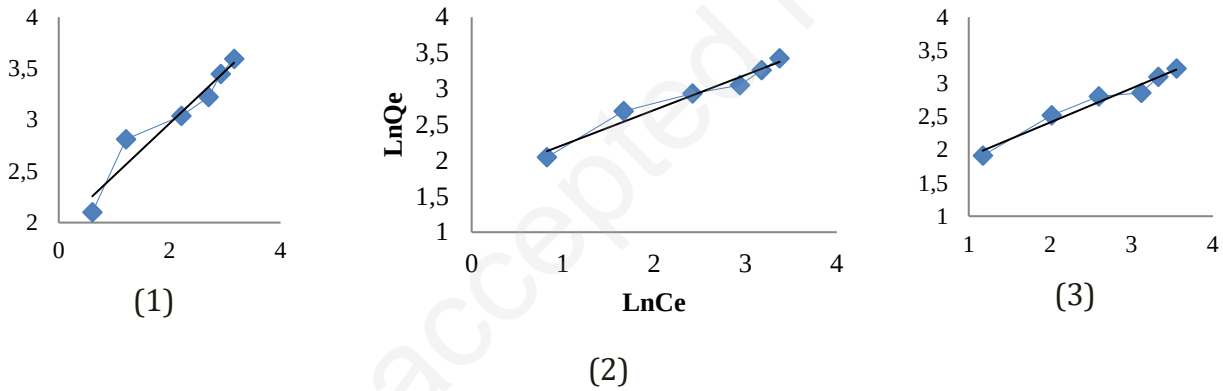

Figure 4. The equilibrium adsorption isotherm based on Freundlich model for the CBZ adsorption on the MWCNT in 303 (1), 308 (2), and 318 (3) K temperatures, respectively.

The Freundlich model data based on its equation and plots are given in Table 3. The magnitude of the lnK_F value and the experimental dimensionless parameter ($\frac{1}{n}$) show that adsorption of the CBZ drug from aqueous solution onto the MWCNT occurred with high capacity and and in a convenient manner. The $\frac{1}{n}$ value is higher than unity for all three temperatures, which means that the CBZ adsorption is favorable. The maximum value of the K_F (mg g^{-1}) for the CBZ drug is in 303 K; this shows that the strong adsorption of the CBZ drug on the MWCNTs. These results are in good agreement with Langmuir model.

Table 3. Carbamazepine (CBZ) surface adsorption parameters based on Freundlich model.

Temperature	R^2	n	K_F
303	0.932	1.97	7.02
308	0.962	2.05	5.63
318	0.963	1.95	4.00

Temkin model

In this model, q_e is plotted against ln C_e to use the slope and intercept to obtain the equilibrium binding constant (A) and Temkin isotherm constant (b), respectively, see Figure 5. The results calculated from these plots are summarized in Table 4. As can be seen in this table, the positive value of the b at all temperatures indicates that the interactions between the CBZ and MWCNT are exothermic. The comparison of the results at these temperatures shows that the best values of the b and the A is 303 K. According to this table, the minimum standard deviation value for these plots is related to 303 K. These results are in good agreement with Langmuir and Freundlich models. So, it may indicate that 303 K is a favorable temperature for the adsorption of CBZ on MWCNT.

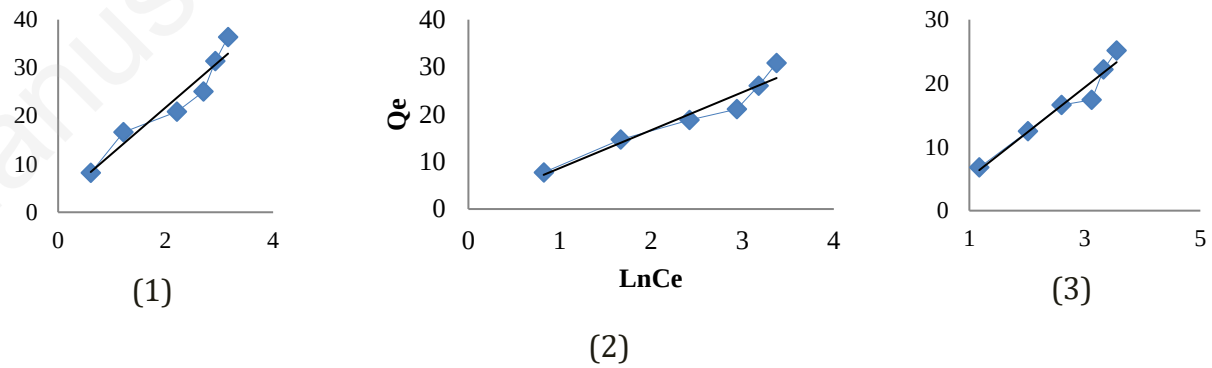

Figure 5. The equilibrium adsorption isotherm based on Temkin model for the CBZ adsorption on the MWCNT in 303 (1), 308 (2), and 318 (3) K temperatures, respectively.

Table 4. The CBZ surface adsorption parameters based on Temkin model.

Temperature	R^2	b	A	SD
303	0.925	9.62	1.30	0.3342
308	0.935	8.02	1.08	0.4229
318	0.946	7.13	0.760	0.7863

The effect of pH in the CBZ adsorption on MWCNT

The pH parameter is classified as an important and effective factor in the CBZ adsorption on MWCNT to get a better insight into the adsorption process. The use of dilute HCl (0.1 mol L^{-1}) and NaOH (0.1 mol L^{-1}) is used to control the pH value. The adsorption value is studied for the CBZ in 30 and 60 mg L^{-1}, see Table 5 and Figure 6. The maximum adsorption of the CBZ onto MWCNT is seen at acidic pH (pH= 2.0). The decrease in the CBZ adsorption value at high pH is mainly due to the cleavage of the aromatic ring of the CBZ ring and generating hydrogen ion. So, an increasing pH leads to a decrease in the adsorption of the CBZ drug.

Table 5. The CBZ adsorption onto MWCNT in different pH.

	pH					
Concentration	**2**	**4**	**6**	**8**	**10**	**12**
30	21.84	20.73	19.90	9.08	5.25	3.33
60	44.35	35.45	35.26	26.38	24.35	22.81

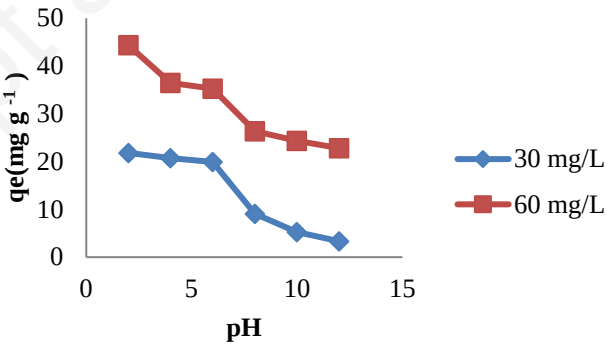

Figure 6. Plot of changing of the CBZ adsorption vs. pH.

The effect of the CBZ concentration on adsorption isotherms

One of the other effective parameters in the CBZ drug adsorption on MWCNT is the CBZ concentration in the solution. MWCNT has a high ability and capacity for the CBZ adsorption

due to its high surface area to volume. Therefore, it seems that high concentration leads to high CBZ adsorption. To confirm this fact, the adsorption value of the CBZ is studied with increasing concentration and constant MWCNT concentration in solution, see Table 6. According this table, increasing the CBZ concentration leads to increasing adsorption value with constant MWCNT concentration.

Table 6. Adsorption value of the CBZ drug on MWCNT at different temperatures.

Concentration	303	308	318
20	16.63	14.71	12.47
30	20.86	18.78	16.58
40	25.08	21.10	17.40
50	31.40	26.02	22.16
60	36.40	30.83	25.16

The effect of temperature and thermodynamic studies

The decreasing in the CBZ adsorption value with increasing temperature indicates that the CBZ adsorption on MWCNT is an exothermic process. By studying the temperature effect on the CBZ adsorption, the thermodynamic parameters can be investigated using following equations:

$$\ln K_F = -\frac{\Delta H}{RT} + \frac{\Delta S}{R} \quad (5)$$

$$\Delta G = -RTlnK_F \quad (6)$$

$$\Delta S = \Delta H - \frac{\Delta G}{T} \quad (7)$$

In these equations, ΔG, ΔH, ΔS, R, T are Gibbs free energy, enthalpy, entropy, universal constant of ideal gas, and temperature [23]. Thermodynamic parameters are calculated to determine the thermodynamic feasibility and spontaneous character of the process. According to equation 2 and plotting of K_F vs. $\frac{1}{T}$ can calculated ΔH and ΔS parameters, see Figure 7 and Table 7. According to this table, the K_F decreases with increasing temperature means that the CBZ adsorption on MWCNT is an exothermic process. Negative value of the ΔH at all temperatures

confirm that the CBZ adsorption on MWCNT is physical adsorption. Moreover, the low negative value of entropy shows that the CBZ is arranged more regularly in binding position. On the other hand, negative value of the ΔG decreases with increasing temperature; indicating un-favorable adsorption.

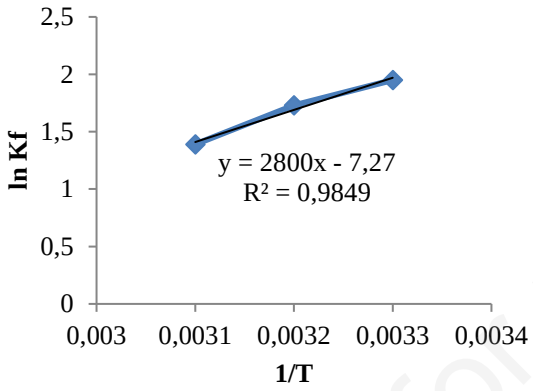

Figure 7. Plot of K_F vs. $\frac{1}{T}$ for the CBZ adsorption on MWCNT at 303, 308, and 318 K.

Table 7. Thermodynamic parameters, ΔG (kJ mol^{-1}), ΔH (kJ mol^{-1}), and ΔS (J mol^{-1} K^{-1}) for the CBZ adsorption on MWCNT at different temperatures

Temperature	$ln\ K_F$	ΔG	ΔH	ΔS
303	1.95	-4.91	-23.3	-60.69
308	1.73	-4.43		-61.27
318	1.39	-3.62		-60.73

The effect of contact time and adsorption kinetics

Investigating chemical kinetic results to accurately understand the effective parameters for the rate of chemical reactions. The plot of q_e vs. time at 20, 30, and 40 mg L^{-1} is shown in Figure 8. According to this figure, the q_e value increases gradually up to 90 minutes, at which time they all reach a steady state called the equilibrium state. Reaching the equilibrium state after 90 min shows that the adsorption kinetic is fast. Chemical kinetic is a detailed study of the conditions that are effective for the rate of chemical reactions [26]. To achieve this, the instant equilibrium

concentration (C_{ie}) of the CBZ drug was measured in each time. Then, instant adsorption capacity (q_t) was calculated by following equation:

$$q_t = \frac{(C_0 - C_{ie})V}{w} \quad (8)$$

All data were fitted by the pseudo-first order and the pseudo-second-order models [12,13]

$$\ln(q_e - q_t) = lnq_e - k_1 t \quad (9)$$

$$\frac{t}{q_t} = \frac{1}{k_2 q_e^2} + \frac{t}{q_e} \quad (10)$$

In these equations, the rate constants of pseudo-first order (k_1) and pseudo-first order adsorptions (k_2) are given in $\frac{1}{min}$ and $\frac{min.gr}{mg}$, respectively. Besides, q_t and q_e are instant and equilibrium adsorption capacities, respectively. In fact, these models examine the adsorption process based on their curves. Plotting $\ln(q_e - q_t)$ vs t and $\frac{t}{q_t}$ vs. t gives k_1 and k_2, respectively, see Figure 9. All kinetic data are listed in Table 8. Comparision of the correlation coefficient (R^2) shows that the k_1 value increases with the CBZ drug concentration. This issue is in good agreement with Langmuir model.

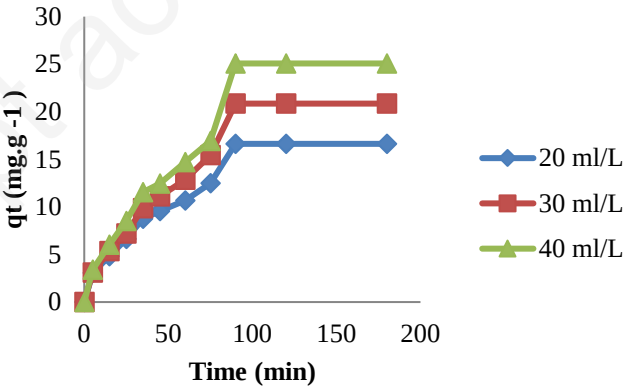

Figure 8. Plotting of concentration on surface adsorption kinetic of the CBZ on MWCNT at 20, 30, and 40 concentrations.

Table 8. pseudo-first order and pseudo-second order parameters of the CBZ adsorption process on MWCNT.

	first order	**second order**

Concentration	q_e	k_1	R^2	k_2	R^2
20	16.63	0.014	0.989	0.030	0.946
30	20.86	0.016	0.987	0.022	0.908
40	25.08	0.016	0.995	0.023	0.941

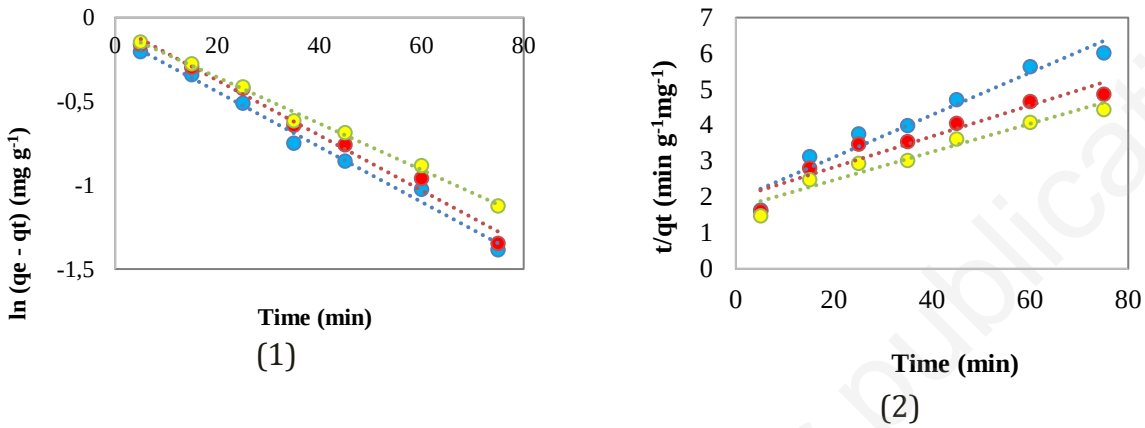

Figure 9. Plotting pseudo-first order and pseudo-second order adsorption of the CBZ drug on MWCNT (blue, red, and yellow colors for 20, 30, and 40 mg L^{-1} concentration)

Conclusions

In conclusion, adsorption of the Carbamazepine (CBZ) drug on MWCNT at 303 K is the most favorable temperature among studied temperatures in this study. Our results show that the best concentration of the CBZ drug adsorption on MWCNT is 60 mg L^{-1} at acidic pH (pH=2). More negative thermodynamic parameters (ΔG, ΔH, and ΔS) show that the CBZ adsorption process is exothermic. The kinetic parameters showed that the physical CBZ adsorption follows a pseudo-first order process. These issues confirm that the CBZ adsorption on MWCNT is favorable. Therefore, it can be concluded the interaction of drug with other organs and side effects are low.

Conflicts of Interests

There are no conflicts of interest.

Acknowledgment

The author's high thank from Dr Fazlolah Eshghi due to high his hint and useful help. In

addition, the authors thank Mahoor Milati for assistance with costs.

Author Contributions

Dr. Mahdi Vadi conceived of the presented idea. Mr. Majid Mohammadi developed the theory, performed the computations, directed the project, suggested the probable mechanism edited and revised the manuscript, Mrs. Narges Bagheri, Khadijeh Shekoohi, and Floura Younessi carried out the analytical method and experiments.

References

1. Eshghi, F., Ghahramani, Z., Ghoreishi, R. & Ghahremani, S. Improvement of floxuridine anti-cancer adsorption on boron carbonitride nanotubes with iron doping: a theoretical study. *Theor. Chem. Acc.* **140**, 119 (2021).
2. Jorshari, M. R., Mamaghani, M. & Jahanshahi, P. Synthesis, delivery, and molecular docking of fused quinolines as inhibitor of Hepatitis A virus 3C proteinase. *Sci. Rep.* **11**, 18970 (2021).
3. Esmaeili, S., Samadizadeh, M. & Khaleghian, M. Evaluating role of the x–π (x = π and/or CH) stacking interactions in adsorption of the (4E,4E)-4-(4-hydroxyphenyldiazenyl)-N-((furan-2-Yl)methylene)benzenamine antibacterial in armchair boron nitride nanotube. *Chem. Pap.* **74**, 2991–3000 (2020).
4. Eshghi, F. & Eshghi, H. Influence sandwich π–π stacking interactions in Benzaldoxime adsorption on the fullerene. *Fullerenes, Nanotub. Carbon Nanostructures* **29**, 227–231 (2021).
5. Eshghi, F. *et al.* Photocatalytic degradation of remdesivir nucleotide pro-drug using [Cu(1-methylimidazole)4(SCN)2] nanocomplex synthesized by sonochemical process: Theoretical, hirshfeld surface analysis, degradation kinetic, and thermodynamic studies. *Environ. Res.* **222**, 115321 (2023).
6. Ghoreishi, R. & Kia, M. Chemical reactivity and adsorption properties of pro-carbazine anti-cancer drug on gallium-doped nanotubes: a quantum chemical study. *J. Mol. Model.*

25, 46 (2019).

7. Prajapati, S. K., Malaiya, A., Kesharwani, P., Soni, D. & Jain, A. Biomedical applications and toxicities of carbon nanotubes. *Drug Chem. Toxicol.* **45**, 435–450 (2022).

8. Yang, Z. *et al.* Pharmacological and toxicological target organelles and safe use of single-walled carbon nanotubes as drug carriers in treating Alzheimer disease. *Nanomedicine Nanotechnology, Biol. Med.* **6**, 427–441 (2010).

9. Wang, R., Zhang, D. & Liu, C. DFT study of the adsorption of 2,3,7,8-tetrachlorodibenzo-p-dioxin on pristine and Ni-doped boron nitride nanotubes. *Chemosphere* **168**, 18–24 (2017).

10. Zhu, W. *et al.* Multi-walled carbon nanotube-based systems for improving the controlled release of insoluble drug dipyridamole . *Exp Ther Med* **17**, 4610–4616 (2019).

11. Guo, Q., Shen, X., Li, Y. & Xu, S. Carbon nanotubes-based drug delivery to cancer and brain. *Curr. Med. Sci.* **37**, 635–641 (2017).

12. Nagai, H. *et al.* Diameter and rigidity of multiwalled carbon nanotubes are critical factors in mesothelial injury and carcinogenesis. *Proc. Natl. Acad. Sci.* **108**, E1330–E1338 (2011).

13. Moayyedi, P. *et al.* Pantoprazole to Prevent Gastroduodenal Events in Patients Receiving Rivaroxaban and/or Aspirin in a Randomized, Double-Blind, Placebo-Controlled Trial. *Gastroenterology* **157**, 403-412.e5 (2019).

14. Li, W. *et al.* Discovery of Novel Quinoline–Chalcone Derivatives as Potent Antitumor Agents with Microtubule Polymerization Inhibitory Activity. *J. Med. Chem.* **62**, 993–1013 (2019).

15. Del Río Castillo, A. E., De León-Rodriguez, A., Terrones, M. & Barba de la Rosa, A. P. Multi-walled carbon nanotubes enhance the genetic transformation of Bifidobacterium longum. *Carbon N. Y.* **184**, 902–909 (2021).

16. Li, D., Xiao, S. & Huang, C. Pharmacia and biological functionalities of nutrient broth dispersed multi-walled carbon nanotubes: A novel drug delivery system. *Sci. China Chem.* **53**, 612–618 (2010).

17. Roohi, H., Nowroozi, A.-R. & Eshghi, F. The gas phase hydrogen-bonded dimers of HOCl: A high-level quantum chemical study. *Int. J. Quantum Chem.* **110**, 1489–1499 (2010).

18. AH. Pakiari, F. E. Geometric and Electronic Structures of Vanadium Sub-nano Clusters, Vn (n = 2-5), and their Adsorption Complexes with CO and O2 Ligands: A DFT-NBO Study. *Phys. Chem. Res,* **5**, 601–615 (2017).

19. Roohi, H., Nowroozi, A., Bavafa, S., Akbary, F. & Eshghi, F. Interaction between NH 2 NO and H 2 O 2 : A quantum chemistry study. *Int. J. Quantum Chem.* NA-NA (2009) doi:10.1002/qua.22364.

20. Roohi, H., Nowroozi, A.-R., Ebrahimi, A., Eshghi, F. & Ahmadepour, E. Influence of HOCl…O 3 and HOCl…HOCl interactions on the stability of O 3 (HOCl) 2 complexes: a theoretical study. *Mol. Simul.* **37**, 386–393 (2011).

21. Zahra Tolou-Ghamari Mohammad Zare, Jafar Mehvari Habibabadi, M. R. N. A quick review of carbamazepine pharmacokinetics in epilepsy from 1953 to 2012. *J Res Med Sci* (2013).

22. Abdelnaeim, M. Y., El Sherif, I. Y., Attia, A. A., Fathy, N. A. & El-Shahat, M. F. Impact of chemical activation on the adsorption performance of common reed towards Cu(II) and Cd(II). *Int. J. Miner. Process.* **157**, 80–88 (2016).

23. Wang, Y., Yang, S.-T., Wang, Y., Liu, Y. & Wang, H. Adsorption and desorption of doxorubicin on oxidized carbon nanotubes. *Colloids Surfaces B Biointerfaces* **97**, 62–69 (2012).

24. by John C. Crittenden, (A.M.ASCE) & Walter J. Weber, Jr., (M.ASCE), Univ. of Michigan, Ann Arbor, M. Model for Design of Multicomponent Adsorption Systems. *Civ. Eng. DATABASE* **104**, 1175–1195 (1978).

25. Sumalinog, D. A. G., Capareda, S. C. & de Luna, M. D. G. Evaluation of the effectiveness and mechanisms of acetaminophen and methylene blue dye adsorption on activated biochar derived from municipal solid wastes. *J. Environ. Manage.* **210**, 255–262 (2018).

26. Al-Johani, H. & Salam, M. A. Kinetics and thermodynamic study of aniline adsorption by multi-walled carbon nanotubes from aqueous solution. *J. Colloid Interface Sci.* **360**, 760–767 (2011).

27. Qiu, H. *et al.* Critical review in adsorption kinetic models. *J. Zhejiang Univ. A* **10**, 716–724 (2009).

28. Ho, Y. S. Review of second-order models for adsorption systems. *J. Hazard. Mater.* **136**,

681–689 (2006).